MAXI Timing Analysis Of The Crab Pulsar

Adam Nawal
Internship Supervisor: Prof. Ken Ebisawa
Academic Advisor: Prof. Hugh Hill

Version 1.2, 14/01/2020

Abstract

The MAXI (Monitor of All-Sky X-ray Image) is an instrument on board the ISS. Operational since late 2009, it has discovered new x-ray sources which have later proven to be fruitful sources of data. Despite this, both timing analysis and barycentric correction remain difficult. A postgraduate researcher produced an easy-to-use barycentric correction tool specifically for use with MAXI, and during the internship period it was tested thoroughly. Once complete, a guide to using common timing tools with MAXI data was produced, and a new tool was written to extract both the period and the spin-down rate of the Crab pulsar from MAXI data. This tool is presented in this report, with a rough figure for the first time derivative of the spin down rate to confirm the fast timing capability of MAXI. These figures were compared with fiducial values taken from the radio astronomy ephemeris maintained by Jodrell Bank. Although the two sets of values roughly agreed, this was to within approximately one millisecond. Since this analysis, a major error has been discovered in the time assignment of MAXI, which could explain the discrepancy.

Acknowledgements

I would like to thank the following people:

My internship supervisor, Professor Ken Ebisawa, for his support, guidance, and advice throughout the internship period.

My academic advisor, Professor Hugh Hill, for supporting and advising me throughout my studies.

The internship co-ordinators, Kristell Bars and Yuko Kadoshima, for arranging the internship despite some bureaucratic difficulties.

My labmates Mayu Tominaga, Reiho Shimomukai, and Takuya Midooka, for being so friendly and welcoming from the outset.

The postgraduate researchers Satoshi Nakahira and Yasuhara Sugawara, for their help, advice, and guidance.

Professor Masahiro Tsujimoto, for his enthusiasm and advice

and the astronomers who maintain the Jodrell Bank crab ephemeris and the MAXI data archive for their tireless work.

Table of Contents

Contents

List of Figures

List of Formula

List of Abbreviations

FFT	Fast Fourier Transform
FITS	Flexible Image Transport System
GSC	Gas Slit Camera
HEASARC	High Energy Astrophysics Science Archive Research Centre
ISAS	Institute of Space and Astronautical Science
ISS	International Space Station
ISU	International Space University
JAXA	Japanese Aerospace Exploration Agency
JEM-EF	Japanese Experiment Module – Exposed Facility
MAXI	Monitor of All-Sky X-ray Image
MJD	Modified Julian Date
NASA	National Aeronautics and Space Administration
NICER	Neutron star Interior Composition ExploreR
RBM	Radiation Belt Monitor
SSC	Solid State Camera

1 Introduction

Launched in 2009, the MAXI telescope was the first addition to the JEM-EF module on the ISS. Completing a full sweep of the sky every 92 minutes, the telescope contains 2 different instruments – the Gas Slit Camera (GSC) and the Solid-State Camera (SSC). The most powerful X-ray all sky monitor when launched, the instruments allow it to see x-rays ranging from 0.5keV up to 30keV. This allows viewing and detection of a wide array of sources, as well as high energy resolution of soft x-rays (Matsuoka et al., 2009).

Despite some initial problems with high-voltage discharges disabling some of the gas slit counters (Sugizaki, 2010), both detectors have performed well in orbit, with the GSC managing a sensitivity of 15 mCrab per day (Sugizaki et al., 2011), and the SSC reaching 50 mCrab per day (Tsunemi et al., 2010). Between them, and the ability of MAXI to produce an unbiased scan of the sky, numerous x-ray sources have been discovered and rediscovered. These results, as well as the ability to work in partnership with the NASA Neutron star experiment NICER (HEASARC: About NICER, 2019), show that MAXI will remain a valuable science tool for some years to come, and so clear and applicable data analysis recipes will be equally valuable.

1.1 Project

The initial project was to test a tool written for barycentric correction of data received by the MAXI telescope. Unreleased as of yet, it was designed to reconcile standard barycentric correction tools with the peculiarities of MAXI – as an all-sky survey, there are large gaps in particular targets. The tool in question was designed to compile the orbit data of short observations of the target into a single orbit file, and then use this file with the existing BARYCEN tool to adjust the detection times of events to their arrival at the solar system barycentre. The output was to be tested against trusted radio astronomy observations from the Jodrell Bank observatory in the UK (Jordan, 2019).

Once this was completed, the project expanded to more general timing analysis of MAXI data. By using the past 10 years of observations of the Crab pulsar, I was to extract the pulse period and the first derivative from MAXI data, and from there produce a guide to be placed on the MAXI website for users of the data to follow. After this, I went on to extract the second time derivative of the period, confirming the fast timing capabilities of MAXI.

1.2 Project Motivation

MAXI is onboard the JEM module of the ISS in low-earth orbit, which is in turn in orbit around the solar system barycentre. Correcting for this motion is essential for accurate timing analysis, as otherwise the events can be smeared out, possibly hiding significant signals and exacerbating noise.

The majority of timing analysis is based on Fourier transform methods, usually the Fast Fourier Transform (FFT). FFT is a powerful tool for finding the frequency of a phenomenon from seemingly random data, but it does not always work well when there are large gaps in the data (Orlandini, 2018). Despite this, it remains at the root of the majority of timing analysis tools used in astronomy today.

Given the nature of MAXI, any given target is only observed for 40 to 100 seconds out of every 92 minute orbit. For analysis of millisecond pulsars such as the Crab pulsar, one orbit's worth of observations may be sufficient, if constrained. For observation of long-term trends, sources with longer periods, or for quasi-periodic oscillations, this hurdle must be overcome. A guide to doing so would be an invaluable addition to the MAXI data analysis guide, making sure that the data was useful for a broad class of users.

For the accuracy required for detailed analysis, barycentric correction is essential. This is the process of adjusting pulse arrival times to the inertial frame of reference of the barycentre of the solar system. This corrects for the orbital motion of both the spacecraft and the Earth. Omitting this causes variation in the arrival times of photons from the target. This leads to a broadening or smearing of pulse peaks, causing errors and potentially hiding weaker signals. A model of barycentric correction is shown in figure 1, below.

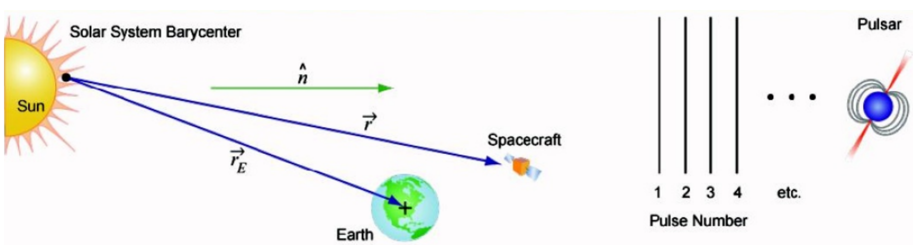

Figure 1: A schematic representation of the principle of barycentric correction (Orlandini, 2018)

1.3 Host institution

The Institute of Space and Aeronautical Science was founded at Tokyo University in 1964. Launching Japan's first artificial satellite in 1970, ISAS later expanded to become a joint venture between Japan's leading universities.

One of the institutions that formed JAXA in 2003, ISAS remains as the space science wing, and is rightly recognised as one of the global leaders in the field of space science and technology. Headquartered at the Sagamihara campus near Tokyo since 1989, ISAS continues to carry out world class research in the fields of astronomy, geophysics, plasma physics, engineering, and cosmology (History | ISAS, 2019).

1.4 Report structure

The first section of this report is an introduction to the project, the motivation for the project, and some background on the host institution. This is followed by the Theory section, which gives a grounding in the physical phenomena being studied and some of the mathematical methods being used. The Methodology section lays out the process engaged in and explains the choices made. The section after that presents the Results, alongside a discussion. The Conclusions and Recommendations follow, summarising the project and recommending areas for further study. Finally, the Evaluation reflects on the experience of the internship and gives advice for future interns.

2 Theory

2.1 Pulsars

First discovered in 1967 by Jocelyn Bell, Pulsars are rapidly rotating compact neutron stars. Often the remnants of a supernova, their rapid and predictable rotation makes them ideal for calibrating the timing of astronomical instruments.

As they rotate, they lose energy as mass radiates away. Because of this, there is a measurable spin-down rate (the first derivative of the period with respect to time, or $\dot{P}$), which measures the speed at which the rotation of the pulsar gradually slows. As rotational energy is lost largely as magnetic dipole radiation, the period and the spin-down rate can put a lower limit on the magnetic field of the pulsar:

$$B \geq 3.3 \times 10^{15} \sqrt{P\dot{P}} \tag{1}$$

where P is measured in seconds, $\dot{P}$ is dimensionless, and B is the magnetic field strength in Teslas. Similarly, the characteristic age of a pulsar (the upper limit of the pulsar's age) can be found as

$$\tau < \frac{1}{2}(\frac{P}{\dot{P}}) \tag{2}$$

with τ being the upper limit of the pulsar's age in years. These values are only limits, and not exact values, as the magnetic field strength also depends on the angle of the magnetic field with the rotational axis (usually unknown), and finding the age of the pulsar requires the initial rotational frequency (also unknown). Nevertheless, these are both useful bounds to characterise the pulsar that can be found from the period and $\dot{P}$(Ryan and Norton, 2010).

One of the most studied pulsars is the Crab pulsar. The remnant of the supernovae that produced the crab nebula and was observed in 1054, the Crab pulsar is one of the brightest objects in the X-ray sky, and is often used for timing calibration. Its behaviour is well known, and plenty of reference data exists – most notably in the form of an Ephemeris produced with radio astronomy data at Jodrell Bank and maintained by the University of Manchester – a table of astronomical data such as observed frequency, first and second time derivatives of frequency, and arrival time of first pulse, updated as new observations arrive (Jordan, 2019).

Glitches

Occasionally, a pulsar will speed up unexpectedly. A glitch is a sudden increase in the frequency of a pulsar, usually of the order of 10^{-3} to 10^{-4} Hz. After this jump, there is a recovery period, with the pulsar period and spin-down rate slowly returning to the pre-glitch level (Pulsar Glitches | Jodrell Bank Centre for Astrophysics, 2019). The cause of glitches is still not fully understood, but current theories indicate that there is a superfluid within the pulsar, rotating faster than the outer, cooler crust. Occasionally these will couple with each other, briefly accelerating the crust and causing the observed increase in frequency. There is a correlation between the characteristic age of a pulsar and glitch frequency – the peak in pulsar glitch activity comes at around 10^4 years, with older pulsars and very young pulsars having glitches very rarely (Espinoza, Lyne, Stappers and Kramer, 2011).

2.2 Timing analysis

Astronomy is principally an observational science. A lot can be learned from spectral analysis or observation, but analysing the variability of a source can be vital to characterising an object.

Finding the frequency of an object's pulsation, or any long-term variability, can be difficult in a noisy spectrum. Fortunately, the Fourier transform is a technique that can decompose a signal into a number of component sine waves of varying frequency and amplitude. For discrete samples of a continuous signal, such that $t_k = k\Delta t$ where $k = 0, 1, 2, \ldots, N-1$ - in other words, for N samples of x_k, each taken at time t_k, the discrete Fourier transform is given by

$$a_j = \sum_{k=0}^{N-1} x_k e^{2i\pi j \frac{k}{N}} \qquad j = \frac{-N}{2}, \ldots, \frac{N}{2} - 1 \tag{3}$$

giving N sine waves. These can be used to plot a power spectrum with the formula

$$P_j \equiv \frac{2}{N_{ph}} |a_j|^2 \qquad j = 0, 1, 2, \ldots, \frac{N}{2} \tag{4}$$

where N_{ph} is the total number of photons received. If there is a sinusoidal signal in the data, the frequency will appear on the power spectrum as a sharp spike, cutting through the noise and allowing the period of the source to be determined (Orlandini, 2018).

The Fast Fourier Transform

As useful as the discrete Fourier transform is, it can be time-consuming to carry out, even on modern computers. Fortunately, algorithms exist to shorten the calculation time significantly. The most common is the Fast Fourier Transform, or FFT.

For a discrete Fourier transform where N is a power of 2, the series can be split in half, such that the even terms are in one new series and the odd terms are in the other:

$$\{x_{1,k}\} = \{x_{2k}\} \qquad k = 0, 1, 2, \ldots, M-1 \, \{x_{2,k}\} = \{x_{2k+1}\} \qquad M = N/2 \quad (5)$$

$$\{x_{2,k}\} = \{x_{2k+1}\} \qquad M = N/2$$

Each has their own fourier transform, which can be combined to get the Fourier transform of the original series:

$$a_j = \sum_{k=0}^{M-1} x_{1,k} e^{2i\pi j \frac{k}{M}} + e^{2i\pi \frac{j}{N}} \sum_{k=0}^{M-1} x_{2,k} e^{2i\pi j \frac{k}{M}} \qquad (6)$$

We can continue to subdivide the input series until M = 1. At this point, $a_j = x_k$, and we can use this to simply sum the terms back up to the Fourier transform of the original series. This is a lot faster, and can be completed in $n \log n$ steps, rather than the n^2 steps the full Fourier transform takes (Orlandini, 2018).

3 Methodology

3.1 Data preparation

The correction and analysis used 5-day observations of the target, centred around the dates given in the Jodrell Bank monthly ephemeris. This allowed a large enough range to ensure the signal would be clearly visible, but was constrained enough to be easy to compare to the radio astronomy data and small enough to work with easily. X-ray observations were not available for every date, however - due to MAXI's position on the ISS, the source was frequently obscured by the Sun, the solar panels of the ISS, or by limitations in the camera's field of view. Double-checking the missing data with data from the RIKEN database confirmed this (MAXI GSC Monitoring of Crab, M1, 2019). The dates where the source was fully or partially occluded, or when observations conditions were poor, are presented in appendix 1.

The limitations of the GSC are laid out by Sugizaki (2010), presenting on behalf of the MAXI team at a conference to celebrate the first year of MAXI data in 2010. The latitudes the GSC can view are shown in figure 2, while the obstructions to the field of view over various orbits are shown in figure 3.

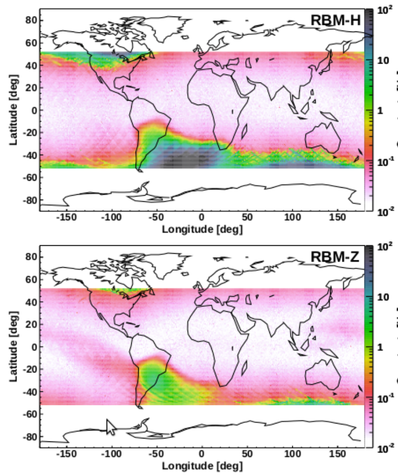

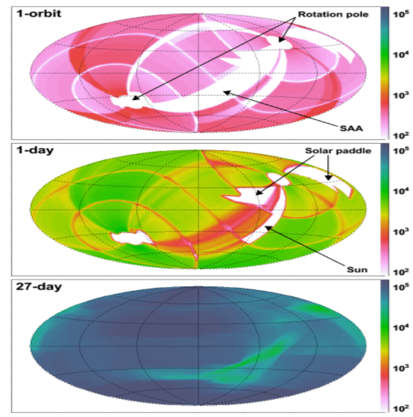

Figure 2: Radiation Belt Monitor count-rate maps of horizon (RBM-H, top panel) and zenith (RBM-Z, bottom panel) units (Sugizaki, 2010)

Figure 3: GSC exposure map by scans of different periods 92-minute orbital period(top), 1 day (middle), and 27 days (bottom) . The color scales of all three panels are identical (Sugizaki, 2010).

The data is in the form of Event files – lists of incident photons, times, channel, and energy. These were extracted using the MXPRODUCT tool, then filtered to only include photons from the source with XSELECT and restricted to 2-4keV to limit background noise as much as possible. After doing so, the barycentric correction tool was used with the data, and both the uncorrected and the newly-created corrected event files were time-sorted, ready for analysis with POWSPEC, which uses the Fast Fourier Transform. Trial and error confirmed that with care, this method was still useful for MAXI data once the event files were time-sorted.

3.2 Analysis

Approximate pulse periods were extracted from both sorted event files with POWSPEC, a tool for extracting a power spectrum from an event file or light curve. Although the Lomb-Scargle algorithm is available in the AstroPy package (and would seem to be better suited to MAXI data), the decision was made to work with POWSPEC, as it is readily available as a part of the XRONOS timing analysis package distributed with FTOOLS, and will therefore be familiar to most researchers. This approximate period was then used as a trial period for EFSEARCH, a tool which folds the event file around the trial period multiple times and returns the most likely period. This period was then compared with the radio astronomy data, both for the corrected and uncorrected files, with the period then used to make a phase-folded curve to compare with the distinctive double-peaked Crab phase curve.

One of the inputs for EFSEARCH is the first derivative of the period (hereafter referred to as $\dot{P}$). The effect of $\dot{P}$ on the output periods was noticeable, with values being taken from the Jodrell Bank ephemeris. In order to check the accuracy, and to analyse how $\dot{P}$ varied over time, a short python script was written to run EFSEARCH multiple times, with a variety of input trial periods and input $\dot{P}$, returning the best period and $\dot{P}$ from those tried. These values were then compared to the radio astronomy data, searching for both a systemic offset and any MAXI-specific timing noise. Fitting a line across the graph of $\dot{P}$ and date, a value was then found for the second time derivative of the period (hereafter referred to as $\ddot{P}$). The script is presented in Appendix 3.

3.2.1 FTOOLS

FTOOLS are a suite of data analysis tools provided by NASA's HEASARC, designed to work with and manipulate FITS files (the standard astronomy data file format). As well as mission-specific calibration files and general image manipulation files, it also contains the flexible and powerful XRONOS timing analysis tools, which were relied on throughout the project - principally POWSPEC, which generates a power spectrum from the input event file, EFSEARCH, which takes an input period and $\dot{\mathrm{P}}$ and searches the event file for the best period near to that, and EFOLD, which takes the input period and produces a phase-folded light curve for the input data. All three tools perform common tasks well, and are well known and routinely used (FTOOLS, 2019).

4 Results and Discussion

4.1 Timing analysis and barycentric correction

After some initial difficulties, as noted in section 3.1, it was possible to carry out a conventional timing analysis using FTOOLS and the barycentric correction script to be tested. Initially, a problem with the script caused the good time intervals of the corrected event files to be mismatched with the updated events. This was soon corrected when reported, and the script worked well. Below in figure 4 is the results of EFSearch with the same data – on the left without barycentric correction, on the right with. Figure 5 is similar, and shows the phase-folded light curves with and without barycentric correction. Full results are presented in appendix 2.

While this proved the barycentric correction script was functioning correctly, when compared to the radio astronomy results, the x-ray data only agreed to within approximately one millisecond. Given the precision required for a lot of timing analysis applications, this was not an encouraging result. However, it did confirm both the period of pulsation of the crab pulsar and the general trend of the pulsar spinning down, which could be built upon.

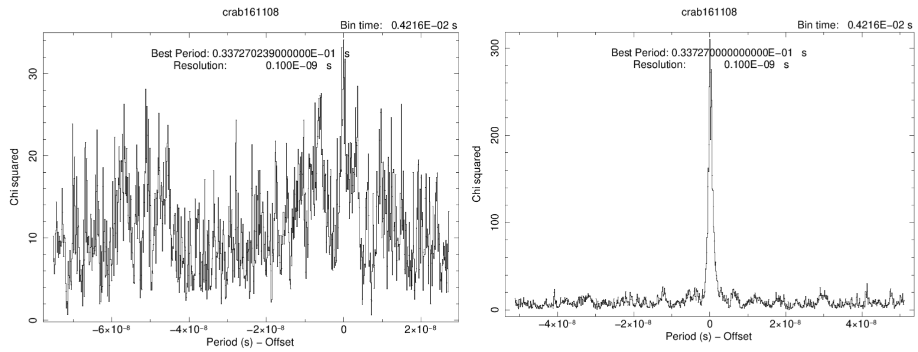

Figure 4: Folded period search with corrected and uncorrected data

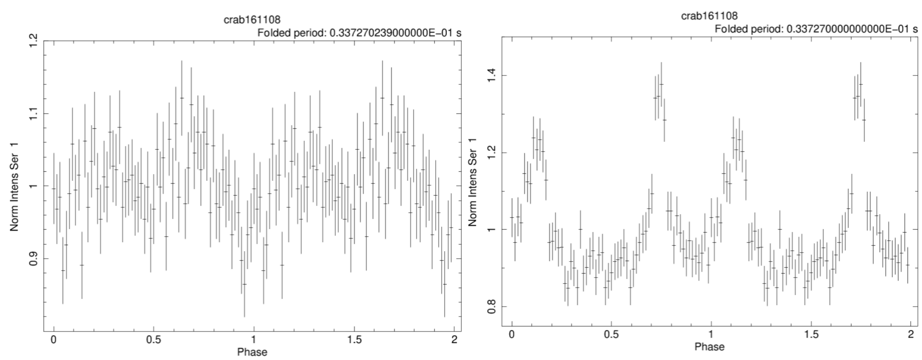

Figure 5: Phase-folded light curve with corrected and uncorrected data
Note the characteristic double peak in the corrected data (right)

4.2 Further analysis results

To obtain the clear results seen above, it was necessary to also take into account the change in period, or $\dot{P}$. This was taken from the Jodrell Bank ephemeris, and matched the radio astronomy data. However, radio waves and x-rays interact differently with the interstellar medium, and so each pulse will have different arrival times in different wavelengths. This offset, as well as other differences like timing resolution, noise, and differences in instrument clock times, could mean that this value for $\dot{P}$ needs to be adapted for MAXI.

To this end, a short script was written (presented in appendix 3) that would take input values of P and $\dot{P}$, take a range of values around the initial estimates, and enter them into EFSearch, taking the best value for the period andproduced. Using this tool, the discrepancy in the period was reduced to the 0.1ms range, with errors in the same vicinity – an improvement, but still quite inaccurate. The value for $\dot{P}$ was found to agree with the radio astronomy results to the order of 1x10^{-16}.

The output of the script was in the form of a contour map, showing the highest chi squared value plotted against the axes of period and $\dot{P}$. An example is below in figure 6. The values of both P and $\dot{P}$ over the period of MAXI's operation are presented in figure 7, alongside the radio astronomy data. The error in the period was calculated from the excess variance in the most accurate EFSearch iteration, taking the standard error of the period as

$$\sigma_{\overline{x}} = \frac{\sigma}{\sqrt{n}} = \frac{\sqrt{var}}{\sqrt{128}} \tag{7}$$

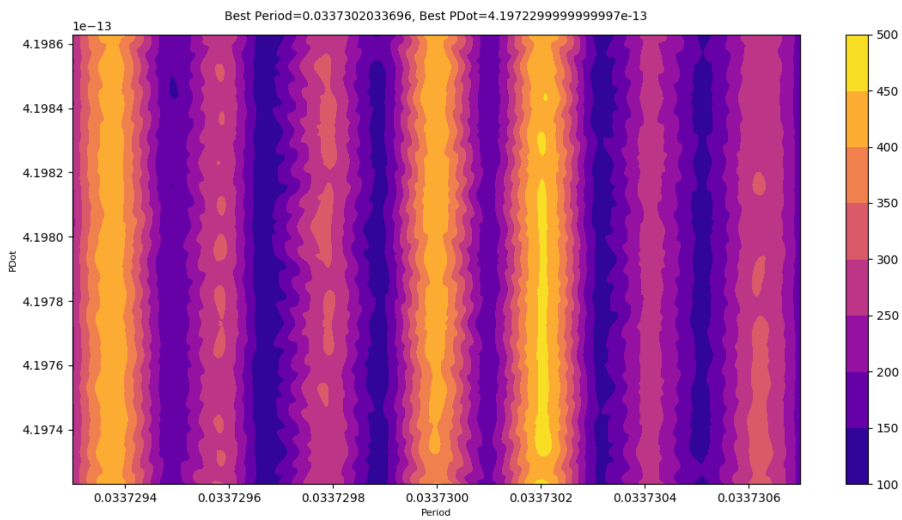

Figure 6: Example output contour map from script written.
Number indicated by colour key is chi squared value of best EFSearch output, with higher values indicating a more significant result.

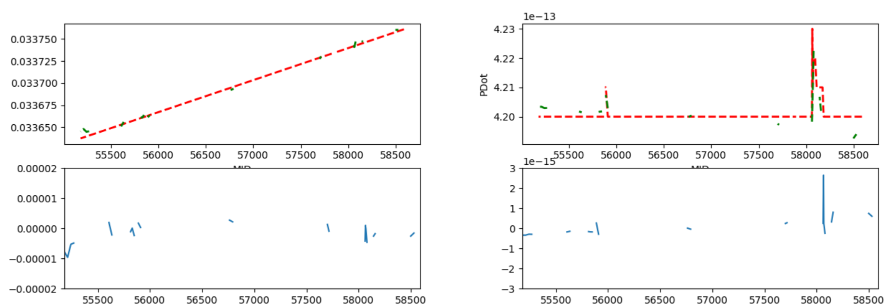

Figure 7: Comparison of data and residuals for period and spin-down rate with Radio Astronomy data.
Shown is the Period (left) and $\dot{P}$ (right) for MAXI data (in green) and the Jodrell Bank radio ephemeris (in red). The bottom graph on both sides show the residuals.

As can be seen, there are gaps in the data for MAXI, due to periods of poor observation conditions. However, there is enough data here to fit a line for $\ddot{P}$. This gives a result of 3.4174x10^{-36}. The radio astronomy data does not have a value for $\ddot{P}$ overall, only monthly values. While there is no figure to directly compare this parameter to, it is useful in assessing how the spin-down rate is expected to change over time.

Of additional interest is the confirmation of the glitches, at MJD 57839 and 58065 (27/03/2017 and 08/11/2017, respectively). This is useful, as it means that future glitches can be confirmed and analysed using MAXI data.

The discrepancies still remain a cause for concern, with the Jodrell Bank ephemeris being given to a precision of $1 \mathrm{x} 10^{-10}$ Hz. Although the timing stability of the GSC has been confirmed to $1 \mathrm{x} 10^{-9}$ (Sugizaki, 2010), I was unable to replicate this level. The script produces event files with a resolution of 50µs, which is more than enough for most timing analysis of astronomical objects.

5 Conclusions and Recommendations

The first conclusion to be drawn is that the barycentric correction script works as desired. When released, it will be valuable for anyone using MAXI data and will allow more accurate timing analysis of any given source over any range of time, regardless of on-source time or gaps in observations.

Secondly, I managed to confirm that MAXI data can be used for timing analysis to a respectable degree of accuracy. Further work may chase down any error or discrepancies as a result of systemic issues with the programs or script used. The offset may be due to difference in clock times between instruments, differences in resolution, or differences in arrival times due to the wavelength-dependent dispersion of photons in the interstellar medium. Another possibility is an error in the time assignment of MAXI. I also produced a short guide for the use of other users of MAXI data, seen in appendix 4.

With that in mind, I would like to make the following recommendations:

• Firstly, MAXI data can and should be used for timing analysis of other sources. Having proven that the technique works on a standard reference source like the Crab pulsar, and with a guide to explain the process, timing analysis of other sources in the X-ray domain could be useful, without having to use an instrument with a specific pointing to observe them

• Secondly, it would also be a useful project to build and maintain a full ephemeris for the Crab pulsar, to compare with the Jodrell Bank ephemeris and see how evolution of the pulsar may differ in the X-ray and Radio domains.

• Finally, one major cause of the offset may be an error in MAXI's time assignment. Once this issue has been resolved, the analysis can be repeated and hopefully show an improvement in results.

6 Evaluation of internship

My experience at JAXA was a valuable one. My previous astronomy experience was in optical astronomy, so learning the differences with x-ray astronomy was a beneficial experience in its own right. I had little experience of timing analysis in this depth, so the experience and knowledge gained of the techniques involved was also quite valuable.

The lab and institute very much encouraged independent working, with supervision and advice coming mostly from the weekly meetings with my supervisor, or the biweekly lab meetings. Being part of this environment and working in this way helped to shape my self-reliance and ability to direct my own work, and being able to work on and contribute to real science was useful.

My supervisor and labmates were all extremely welcoming and supportive, throwing me a welcome party on arrival and getting to know me. I knew little about the culture or area, and knew nobody nearby, so this tradition was extremely helpful in getting me settled.

My advice for any future interns visiting the Sagamihara campus from ISU would be to embrace the culture, the area, and to take full advantage of the opportunities presented. There are regular colloquia and coffee chats on a variety of topics, as well as valuable opportunities to network often. Staying in the on-campus visiting researcher lodge also allowed me to make contact with a number of other interns from across the world, and was extremely affordable (as well as being very close to the workplace), so it is also highly advised.

As well as education, take the opportunity to see and learn about Japan. Sagamihara is an hour from Shinjiku station in Tokyo by regular train, and the bullet train can take you to all over the country quickly, so make sure to take advantage of any opportunities you get to have new experiences.

References

[1] Espinoza, C., Lyne, A., Stappers, B. and Kramer, M., 2011. A study of 315 glitches in the rotation of 102 pulsars. Monthly Notices of the Royal Astronomical Society, 414(2), pp.1679-1704.

[2] Heasarc.gsfc.nasa.gov. 2019. FTOOLS. [online] Available at: <http://heasarc.gsfc.nasa.gov/ftools> [Accessed 29 November 2019].

[3] Heasarc.gsfc.nasa.gov. 2019. HEASARC: About NICER. [online] Available at: <https://heasarc.gsfc.nasa.gov/docs/nicer/nicer_about.html> [Accessed 25 November 2019].

[4] History. 2019. History ISAS. [online] Available at: <http://www.isas.jaxa.jp/en/about/history/> [Accessed 29 November 2019].

[5] Jb.man.ac.uk. 2019. Pulsar Glitches | Jodrell Bank Centre For Astrophysics. [online] Available at: <http://www.jb.man.ac.uk/pulsar/glitches.html> [Accessed 29 November 2019].

[6] Jordan, C., 2019. Jodrell Bank Observatory: Crab Pulsar Monthly Ephemeris | Jodrell Bank Centre For Astrophysics. [online] Jb.man.ac.uk. Available at: <http://www.jb.man.ac.uk/pulsar/crab.html> [Accessed 25 November 2019].

[7] Matsuoka, M., Kawasaki, K., Ueno, S., Tomida, H., Kohama, M., Suzuki, M., Adachi, Y., Ishikawa, M., Mihara, T., Sugizaki, M., Isobe, N., Nakagawa, Y., Tsunemi, H., Miyata, E., Kawai, N., Kataoka, J., Morii, M., Yoshida, A., Negoro, H., Nakajima, M., Ueda, Y., Chujo, H., Yamaoka, K., Yamazaki, O., Nakahira, S., You, T., Ishiwata, R., Miyoshi, S., Eguchi, S., Hiroi, K., Katayama, H. and Ebisawa, K., 2009. The MAXI Mission on the ISS: Science and Instruments for Monitoring All-Sky X-Ray Images. Publications of the Astronomical Society of Japan, 61(5), pp.999-1010.

[8] Maxi.riken.jp. 2019. MAXI GSC Monitoring Of Crab, M 1. [online] Available at: <http://maxi.riken.jp/pubdata/v6l/J0534+220/index.html> [Accessed 25 November 2019].

[9] Orlandini, M., 2018. Temporal Data Analysis: Theory And Procedures. 2nd ed.

[10] Ryan, S. and Norton, A., 2010. Stellar Evolution And Nucleosynthesis. Cambridge: Cambridge University Press.

[11] Sugizaki, M., 2010. Status of Calibration and Data Analysis of MAXI GSC. In: The First Year of MAXI : Monitoring variable X-ray sources. [online] Available at: <http://maxi.riken.jp/FirstYear/> [Accessed 25 November 2019].

[12] Sugizaki, M., Mihara, T., Serino, M., Yamamoto, T., Matsuoka, M., Kohama, M., Tomida, H., Ueno, S., Kawai, N., Morii, M., Sugimori, K., Nakahira, S., Yamaoka, K., Yoshida, A., Nakajima, M., Negoro, H., Eguchi, S., Isobe, N., Ueda, Y. and Tsunemi, H., 2011. In-Orbit Performance of MAXI Gas Slit Camera (GSC) on ISS. Publications of the Astronomical Society of Japan, 63(sp3), pp.S635-S644.

[13] Tsunemi, H., Tomida, H., Katayama, H., Kimura, M., Daikyuji, A., Miyaguchi, K., Maeda, K. and Maeda, K., 2010. In-Orbit Performance of the MAXI/SSC onboard the ISS. Publications of the Astronomical Society of Japan, 62(6), pp.1371-1379.

Appendix 1 - Obscured and Occluded Observations

Start date (MJD)	Start date	End date (MJD)	End date	Comment
58689	25/07/19	58693	29/07/19	Obscured
58647	13/06/19	58651	17/06/19	Obscured
58616	13/05/19	58620	17/05/19	Obscured
58555	13/03/19	58559	17/03/19	Partially obscured
58474	22/12/18	58478	26/12/18	Obscured
58459	07/12/18	58463	11/12/18	Partially obscured
58404	13/10/18	58408	17/10/18	Obscured
58312	13/07/18	58316	17/07/18	Partially obscured
58282	13/06/18	58286	17/06/18	Obscured
58251	13/05/18	58255	17/05/18	Bad observation conditions
58183	06/03/18	58187	10/03/18	Partially obscured
58171	22/02/18	58175	26/02/18	Obscured
58109	22/12/17	58113	26/12/17	Partially obscured
58066	09/11/17	58070	13/11/17	Bad observation conditions
58039	13/10/17	58043	17/10/17	Partially obscured
58009	13/09/17	58013	17/09/17	Bad observation conditions
57917	13/06/17	57921	17/06/17	Obscured
57886	13/05/17	57890	17/05/17	Partially obscured
57825	13/03/17	57829	17/03/17	Obscured
57735	13/12/16	57739	17/12/16	Partially obscured
57674	13/10/16	57678	17/10/16	Bad observation conditions
57644	13/09/16	57648	17/09/16	Bad observation conditions
57613	13/08/16	57617	17/08/16	Partially obscured
57552	13/06/16	57556	17/06/16	Obscured
57521	13/05/16	57525	17/05/16	Obscured
57491	13/04/16	57495	17/04/16	Bad observation conditions

55574	13/01/11	55578	17/01/11	Partially obscured
57460	13/03/16	57464	17/03/16	Bad observation conditions
57431	13/02/16	57435	17/02/16	Bad observation conditions
57308	13/10/15	57312	17/10/15	Obscured
57247	13/08/15	57251	17/08/15	Obscured
57216	13/07/15	57220	17/07/15	Bad observation conditions
57186	13/06/15	57190	17/06/15	Obscured
57094	13/03/15	57098	17/03/15	Partially obscured
57035	13/01/15	57039	17/01/15	Obscured
56943	13/10/14	56947	17/10/14	Partially obscured
56882	13/08/14	56886	17/08/14	Bad observation conditions
56851	13/07/14	56855	17/07/14	Bad observation conditions
56821	13/06/14	56825	17/06/14	Obscured
56729	13/03/14	56733	17/03/14	Obscured
56670	13/01/14	56674	17/01/14	Obscured
56578	13/10/13	56582	17/10/13	Partially obscured
56548	13/09/13	56552	17/09/13	Bad observation conditions
56517	13/08/13	56521	17/08/13	Bad observation conditions
56456	13/06/13	56460	17/06/13	Obscured
56364	13/03/13	56368	17/03/13	Partially obscured
56305	13/01/13	56309	17/01/13	Partially obscured
56213	13/10/12	56217	17/10/12	Bad observation conditions
56183	13/09/12	56187	17/09/12	Bad observation conditions
56152	13/08/12	56156	17/08/12	Bad observation conditions
56091	13/06/12	56095	17/06/12	Obscured
56060	13/05/12	56064	17/05/12	Bad observation conditions
55999	13/03/12	56003	17/03/12	Partially obscured
55939	13/01/12	55943	17/01/12	Bad observation conditions
55876	11/11/11	55880	15/11/11	Partially obscured
55873	08/11/11	55877	12/11/11	Partially obscured
55868	03/11/11	55872	07/11/11	Bad observation conditions
55786	13/08/11	55790	17/08/11	Partially obscured
55725	13/06/11	55729	17/06/11	Obscured
55664	13/04/11	55668	17/04/11	Partially obscured
55452	13/09/10	55456	17/09/10	Obscured
55360	13/06/10	55364	17/06/10	Obscured
55299	13/04/10	55303	17/04/10	Bad observation conditions

Appendix 2 - Full Results

Start	End	Centre	F (JB)	$\dot{F}(\mathrm{e}^{-15})$	$\dot{P}$	MAXI P (s)	Error	Offset	MAXI$\dot{P}$	Offset
58586	58590	58588	29.6200	-368446.48	4.1996E-13	0.03376146	9.7201E-04	-5.4176E-07	4.20271E-13	-3.1526E-16
58527	58531	58529	29.6219	-368513.73	4.1998E-13	0.03376035	8.4266E-04	-1.5670E-06	4.19401E-13	5.7555E-16
58496	58500	58498	29.6229	-368538.75	4.1998E-13	0.03376025	8.5323E-04	-2.5921E-06	4.19257E-13	7.1955E-16
58435	58439	58437	29.6249	-368618.75	4.2001E-13	0.03375537	3.3283E-04	7.2842E-08	4.20106E-13	-9.4752E-17
58221	58225	58223	29.6317	-369005.25	4.2027E-13	0.03375043	1.3003E-03	-2.7593E-06	4.20218E-13	4.9987E-17
58155	58159	58157	29.6338	-369362.12	4.2061E-13	0.03374705	6.2133E-04	-1.7707E-06	4.20198E-13	4.0999E-16
58140	58144	58142	29.6343	-369489.49	4.2074E-13	0.03374732	5.2060E-04	-2.5901E-06	4.2068E-13	5.9832E-17
58077	58081	58079	29.6363	-370857.08	4.2224E-13	0.03374708	1.9460E-03	-4.6371E-06	4.22244E-13	-5.3671E-18
58066	58070	58068	29.6366	-369626.33	4.2083E-13	0.03374197	7.3998E-04	7.2471E-08	4.20765E-13	6.5037E-17
58063	58067	58065	29.6369	-371240.11	4.2265E-13	0.03374104	9.2301E-04	6.3793E-07	4.20357E-13	2.2980E-15
58065	58065	58065	29.6369	-371240.11	4.2265E-13	0.03374070	8.6939E-04	9.7543E-07	4.20357E-13	2.2980E-15
58059	58063	58061	29.6368	-368616.01	4.1967E-13	0.03374603	1.2711E-04	-4.2288E-06	4.19746E-13	-7.4758E-17
57837	57841	57839	29.6443	-368942.08	4.1983E-13	0.03372999	4.9777E-04	3.3229E-06	4.19678E-13	1.5284E-16
57713	57717	57715	29.6479	-368970.96	4.1977E-13	0.03373020	2.0991E-04	-9.5016E-07	4.19723E-13	4.5387E-17
57698	57702	57700	29.6483	-368981.97	4.1977E-13	0.03372741	4.4653E-04	1.2998E-06	4.19758E-13	1.0387E-17
57491	57495	57493	29.6549	-369189.79	4.1981E-13	0.03372604	1.1117E-03	-4.8370E-06	4.19765E-13	4.5020E-17
57431	57435	57433	29.6568	-369252.11	4.1982E-13	0.03371895	1.0377E-03	7.2912E-08	4.19919E-13	-9.5102E-17
57278	57282	57280	29.6617	-369416.08	4.1987E-13	0.03371586	5.6910E-04	-2.3801E-06	4.19777E-13	9.5470E-17
57216	57220	57218	29.6637	-369473.91	4.1989E-13	0.03372626	1.1563E-03	-1.5034E-05	4.19936E-13	-4.9652E-17
57125	57129	57127	29.6666	-369571.63	4.1991E-13	0.03371498	7.7962E-04	-7.0536E-06	4.19979E-13	-6.4897E-17
57066	57070	57068	29.6685	-369636.52	4.1993E-13	0.03371532	8.8444E-04	-9.5380E-06	4.1993E-13	4.9202E-18
56974	56978	56976	29.6714	-369730.03	4.1996E-13	0.03369564	1.1385E-04	6.8011E-06	4.19991E-13	-3.5263E-17
56913	56917	56915	29.6734	-369771.26	4.1995E-13	0.03369486	1.1200E-03	5.3681E-06	4.19894E-13	5.4798E-17
56790	56794	56792	29.6773	-369912.92	4.2000E-13	0.03369362	2.2428E-04	2.1462E-06	4.20042E-13	-4.4630E-17
56760	56764	56762	29.6783	-369942.92	4.2000E-13	0.03369196	7.1094E-04	2.7202E-06	4.19989E-13	1.5309E-17
56701	56705	56703	29.6802	-370008.05	4.2003E-13	0.03369206	8.7050E-04	4.7988E-07	4.20067E-13	-3.4935E-17
56639	56643	56641	29.6821	-370068.03	4.2004E-13	0.03369205	3.2160E-05	-1.7593E-06	4.20089E-13	-4.9996E-17
56486	56490	56488	29.6870	-370216.46	4.2007E-13	0.03368955	3.3274E-04	-4.8116E-06	4.20029E-13	4.4698E-17
56395	56399	56397	29.6899	-370312.33	4.2010E-13	0.03368520	1.9493E-04	-3.7650E-06	4.20016E-13	8.5454E-17
56336	56340	56338	29.6918	-370369.4	4.2011E-13	0.03367881	8.7356E-04	4.8022E-07	4.20053E-13	5.5393E-17
56274	56278	56276	29.6938	-370430.01	4.2012E-13	0.03367697	9.5348E-04	7.2371E-08	4.20147E-13	-2.4730E-17
56183	56187	56185	29.6967	-370520.93	4.2014E-13	0.03367102	1.7371E-04	2.7161E-06	4.20223E-13	-7.9913E-17
56121	56125	56123	29.6987	-370547.08	4.2012E-13	0.03367264	5.0510E-04	-1.1522E-06	4.20205E-13	-8.9669E-17
56060	56064	56062	29.7007	-370633.95	4.2016E-13	0.03366896	2.4508E-04	3.1312E-07	4.20237E-13	-8.0035E-17
55970	55974	55972	29.7036	-370724.16	4.2018E-13	0.03366655	1.6530E-03	-5.4102E-07	4.2015E-13	3.4720E-17
55908	55912	55910	29.7055	-370843.37	4.2025E-13	0.03366348	6.6795E-04	2.7705E-07	4.20294E-13	-3.9891E-17
55887	55891	55889	29.7062	-371201.98	4.2064E-13	0.03366128	3.2392E-04	1.7083E-06	4.20738E-13	-9.5313E-17
55847	55851	55849	29.7075	-370762.89	4.2011E-13	0.03366393	1.1515E-04	-2.3836E-06	4.20178E-13	-6.9607E-17
55828	55832	55830	29.7081	-370798.13	4.2013E-13	0.03366078	1.4460E-03	7.2638E-08	4.20174E-13	-4.4791E-17

55209	55213	55211	29.7279	-371401.32	4.2025E-13	0.03364802	6.9811E-04	-9.6402E-06	4.20339E-13	-8.4891E-17
55812	55816	55814	29.7086	-370781.92	4.2010E-13	0.03366139	4.5665E-04	-1.1196E-06	4.20161E-13	-5.9546E-17
55755	55759	55757	29.7104	-370843.5	4.2012E-13	0.03365895	4.2513E-04	-7.4596E-07	4.2003E-13	8.5331E-17
55694	55698	55696	29.7124	-370923.26	4.2015E-13	0.03365757	1.4844E-03	-1.5790E-06	4.20185E-13	-3.4974E-17
55633	55637	55635	29.7143	-370976.12	4.2016E-13	0.03365597	4.1368E-04	-2.1957E-06	4.20147E-13	9.9648E-18
55605	55609	55607	29.7152	-371002.52	4.2016E-13	0.03365083	7.9157E-05	1.9280E-06	4.20179E-13	-1.5096E-17
55543	55547	55545	29.7172	-371060.62	4.2017E-13	0.03365497	1.1696E-03	-4.4634E-06	4.20251E-13	-8.0157E-17
55482	55486	55484	29.7192	-371124.25	4.2018E-13	0.03364760	2.3350E-04	6.9048E-07	4.202E-13	-1.5280E-17
55390	55394	55392	29.7221	-371219.32	4.2021E-13	0.03364632	1.7217E-04	-1.3693E-06	4.20257E-13	-4.4524E-17
55329	55333	55331	29.7241	-371288.61	4.2024E-13	0.03364717	5.4575E-04	-4.4282E-06	4.20175E-13	6.5232E-17
55268	55272	55270	29.7261	-371343.16	4.2025E-13	0.03364540	8.8982E-04	-4.8751E-06	4.20297E-13	-4.9830E-17
55240	55244	55242	29.7270	-371370.63	4.2025E-13	0.03364480	4.3081E-04	-5.2975E-06	4.20292E-13	-4.4830E-17
55178	55182	55180	29.7289	-371435.8	4.2027E-13	0.03364503	5.3030E-04	-7.7774E-06	4.20338E-13	-7.0013E-17

Appendix 3 - DPDot finder tool

```
#import all necessary
import argparse
import subprocess
import matplotlib.pyplot as plt
from matplotlib import cm
import numpy as np
import astropy.io.fits as fits
import scipy.interpolate
from astropy.table import Table, Column
#take arguments
parser = argparse.ArgumentParser()
parser.add_argument("filename", help="The event file or light curve
    to analyse")
parser.add_argument("period", help="The initial period to try analysing
    around", type=float)
parser.add_argument("pdiff", help="How much to increment the
    trial period by", type=float)
parser.add_argument("dpdot", help="The initial first derivative of
    the period to try analysing around", type=float)
parser.add_argument("dpdiff", help="How much to increment the
    trial first derivative by", type=float)
```

parser.add_argument("--trials", help="The number of iterations to try for each variable. Default is 7. Please note that this is iterated over twice, so the number of trials is the square of the number you enter.", default=7, type=int)

parser.add_argument("--cleanup", help="Whether DpdotFind should delete temporary files created during subroutines. Default is TRUE.", default=True, type=bool) parser.add_argument("--outfile", help="Name of the output file to be created. Default is Results.", default="results")

args=parser.parse_args()

infile = args.filename

period = args.period

pdiff = args.pdiff

dpdot = args.dpdot

dpdiff = args.dpdiff

trials = args.trials

cleanup = args.cleanup

outfile = args.outfile

#Get info for output header

fil = fits.open(infile)

filehead = fil[1].header

TimeA = ("DATE-OBS", filehead["DATE-OBS"], filehead.comments["DATE-OBS"])

TimeB = ("TIME-OBS", filehead["TIME-OBS"], filehead.comments["TIME-OBS"])

TimeC = ("DATE-END", filehead["DATE-END"], filehead.comments["DATE-END"])

TimeD = ("TIME-END", filehead["TIME-END"], filehead.comments["TIME-END"])

RA = ("RA", filehead["RA_NOM"], filehead.comments["RA_NOM"])

DEC = ("DEC", filehead["DEC_NOM"], filehead.comments["DEC_NOM"])

fil.close()

#iterate efsearch

if trials%2==0:

dpinit = dpdot - (trials/2 - 0.5)*dpdiff

pinit = period - (trials/2 - 0.5)*pdiff

else:

```
dpinit = dpdot - (trials//2)*dpdiff
pinit = period - (trials//2)*pdiff
rows=[]
subprocess.call("mkdir DPDotTmp", shell=True)
for i in range(trials):
dptry = dpinit + i*dpdiff
for j in range(trials):
periodtry = pinit + j*pdiff
efs = "efsearch "+infile+" window='-' sepoch=INDEF dper="+str(periodtry)+"
    nphase=INDEF nbint=INDEF dres="+str(pdiff/128)+" nper=128
    outfile=DPDotTmp/dpdot"+str(i)+str(j)+".fes plot=NO dpdot="+str(dptry)+"
    tchat=3" #command line string
print("Iteration "+ str(i*trials + j+1)+" of "+str(trials**2))
subprocess.call(efs, shell=True) #running EFSearch
t=Table.read("DPDotTmp/dpdot"+str(i)+str(j)+".fes", hdu=1, for-
    mat="fits") #Take table from file
tfil = fits.open("DPDotTmp/dpdot"+str(i)+str(j)+".fes")
#getting variance value for error
var = tfil[1].header["VAROB_1"]
err = np.sqrt(np.absolut(var))/np.sqrt(128)
tfil.close()
t.sort("CHISQRD1") #Sort by Chi2
rows.append([t["PERIOD"][-1], dptry, t["CHISQRD1"][-1], err) #Ap-
    pend values to row
if cleanup==True: #cleanup temp files
subprocess.call("rm -r DPDotTmp", shell=True)
#Create results table and append rows
results = Table(rows=rows, names=["Period", "PDot", "Chi2", "Er-
    ror"])
#output file
Hdu = fits.table_to_hdu(results)
head = Hdu.header
head.set("TUNIT1", "s", before="TTYPE2")
head.append(("INPUT", infile, "Input file path specified"), end=True)
head.append(("PIn", str(period), "Initial test period"), end=True)
head.append(("PDiff", str(pdiff), "Test Period step size"), end=True)
```

```
head.append(("DPDotIn", str(dpdot), "Initial test first derivative"),
    end=True)
head.append(("DPDiff", str(dpdiff), "Test first derivative step size"),
    end=True)
head.append(TimeA, end=True) head.append(TimeB, end=True)
    head.append(TimeC, end=True)
head.append(TimeD, end=True) head.append(RA, end=True) head.append(DEC,
    end=True)
Hdu.name = "Results"
Hdu.writeto(outfile+".dpd", overwrite=True)
#plot contours
results.sort("Chi2")
N=10000
x=(results["Period"])
y=(results["PDot"])
z=(results["Chi2"])
X = np.linspace(pinit, pinit+(trials-1)*pdiff, N)
Y = np.linspace(y.min(), y.max(), N)
Z = scipy.interpolate.griddata((x, y), z, (X[None,:], Y[:,None]), method="cubic",
    rescale=True)
fig, ax = plt.subplots()
CS = ax.contourf (X, Y, Z, cmap="plasma")
ax.set_xlabel("Period", fontsize=8)
ax.set_ylabel("PDot", fontsize=8)
ax.set_title("Best Period="+str(results["Period"][-1])+", Best PDot="+str(results["PDot"][-
    1]), fontsize=10, pad=12) fig.colorbar(CS) plt.show()
#print best values
print("Best Period="+str(results["Period"][-1])+", Best PDot="+str(results["PDot"][-
    1]))
print("Error="+str(results["Error"][-1]))
```

Appendix 4 – Timing Guide

Barycentric Correction

Before analysis can take place, the event files must be corrected for barycentric motion. There is a script available to do this that is specialised for MAXI data. The syntax to use it is

```
python␣-i␣mxbarycorr.py␣--start␣55200␣--stop␣55211␣--target␣target
```

where "start" and "stop" refer to the start and stop dates entered into MXPRODUCT. These can be in the format of MJD, or of YYYY-MM-DD. The target refers to the name given for the object parameter with MXPRODUCT – for example, if you specified

```
object=crab
```

then for this script you would use

```
-target␣crab
```

The script will expect the Products folder to be in the directory it's run from, with the folder named "Products". If you specified a different output path when running MXPRODUCT, simply move and rename the folder, run the script, and then move the folder back to the desired location.

The output of this is a corrected event file called crab_g_low_bary.evt. You can then filter this by region or channel using XSPEC as normal.

Using the Xronos package for timing analysis

It is possible to use the XRONOS tools POWSPEC, EFSEARCH, and EFOLD to extract a precise period from the light curve, or directly from the event file produced by MXPRODUCT. Once the event file has been barycentre corrected, make sure it is in time order with FTSort – for example, you can use

```
ftsort crab_g_low_bary.evt+1 crab_g_low_sort.evt TIME
```

to create a time-sorted event file "crab_g_low_sort.evt". This event file is suitable to use with the XRONOS timing suite, available as a part of HEASOFT. An example of using POWSPEC is given below:

```
powspec cfile1="crab_g_low_sort.evt" window="-" dtnb=1e-3 nbint=8192 nintfm=INDEF
rebin=0 plot=yes plotdev="/xw" outfile="-"
```

This should produce a power spectrum with a clear peak indicating the frequency. This can be used to obtain a trial period to input into EFSEARCH. For example, if the best frequency given by POWSPEC was 29.68 Hz, then you can try

```
efsearch cfile1="crab_g_low_sort.evt" window="-" sepoch=INDEF dper=0.03369
dpdot=4.2e-13 nphase=10 nbint=INDEF nper=128 dres=INDEF outfile="-" plot=yes
plotdev="/xw"
```

Including the dpdot parameter can make a huge difference, especially if your data covers a large observation period. Once a more precise period has been extracted from EFSEARCH, a phase plot can be obtained with EFOLD, like so:

```
efold nser=1 cfile1="myfile.lc" window="-" sepoch=INDEF dper=0.03369678231
dpdot=4.2e-13 nphase=10 nbint=300 nintfm=INDEF plot=yes plotdev="/xw" plotdnum=1
outfile="-"
```